

## Structural basis for ubiquitin recognition by the human ESCRT-II EAP45 GLUE domain

Steven L Alam<sup>1</sup>, Charles Langelier<sup>1</sup>, Frank G Whitby<sup>1</sup>, Sajjan Koirala<sup>1</sup>, Howard Robinson<sup>2</sup>, Christopher P Hill<sup>1</sup> & Wesley I Sundquist<sup>1</sup>

**The ESCRT-I and ESCRT-II complexes help sort ubiquitinated proteins into vesicles that accumulate within multivesicular bodies (MVBs). Crystallographic and biochemical analyses reveal that the GLUE domain of the human ESCRT-II EAP45 (also called VPS36) subunit is a split pleckstrin-homology domain that binds ubiquitin along one edge of the  $\beta$ -sandwich. The structure suggests how human ESCRT-II can couple recognition of ubiquitinated cargoes and endosomal phospholipids during MVB protein sorting.**

Late endosomal compartments called multivesicular bodies serve as primary sorting sites for cell-surface receptors and other membrane proteins that are ultimately downregulated through lysosomal degradation. Ubiquitinated cargoes are sorted into MVB vesicles through the sequential action of three multiprotein complexes called ESCRT-I, ESCRT-II and ESCRT-III<sup>1</sup>. Both human and yeast ESCRT-I complexes bind ubiquitin (Ub) through ubiquitin E2 variant domains of the

TSG101 (yeast Vps23p) subunit<sup>2,3</sup>. In contrast, the human and yeast ESCRT-II complexes must recognize ubiquitin differently, because yeast ESCRT-II binds Ub through the second of two Npl4 zinc finger (NZF) modules embedded within the ‘GRAM-like Ub binding in EAP45’ (GLUE) domain of the Vps36p subunit<sup>4</sup>, whereas the mammalian homolog, EAP45 (or VPS36), binds Ub directly through its GLUE domain<sup>5</sup>.

To learn how human ESCRT-II recognizes ubiquitinated protein cargoes, we determined crystal structures of the EAP45 GLUE–Ub complex (Fig. 1, **Supplementary Methods** and **Supplementary Table 1** online). Like its yeast counterpart<sup>6</sup>, EAP45 GLUE adopts a pleckstrin-homology (PH) domain fold, with a seven-stranded  $\beta$ -sandwich capped by a C-terminal  $\alpha$ -helix (Fig. 1a). The EAP45 and Vps36p GLUE domains are both ‘split’ by insertions within the S6–S7 loop. Split PH domains have been characterized previously<sup>7–9</sup>, but these are the first examples in which the insertion occurs at this position. The 16-residue insertion of EAP45 GLUE forms an exposed loop that buttresses the base of the bound Ub molecule and then extends into solution, whereas the larger insertion within Vps36p (~150 residues) contains two NZF modules that bind ESCRT-I and Ub<sup>4,6</sup>, respectively. The structures of the human EAP45 and yeast Vps36p GLUE domains are otherwise very similar (r.m.s. deviation of 0.77 Å over secondary structure regions), despite sharing just 14% sequence identity (see **Supplementary Figs. 1** and **2** online).

In the complex, the S5 edge of the second sheet of the EAP45 GLUE  $\beta$ -sandwich binds the exposed Ub  $\beta$ -sheet. The Ub interface is centered about Val70 and spans an extended hydrophobic patch

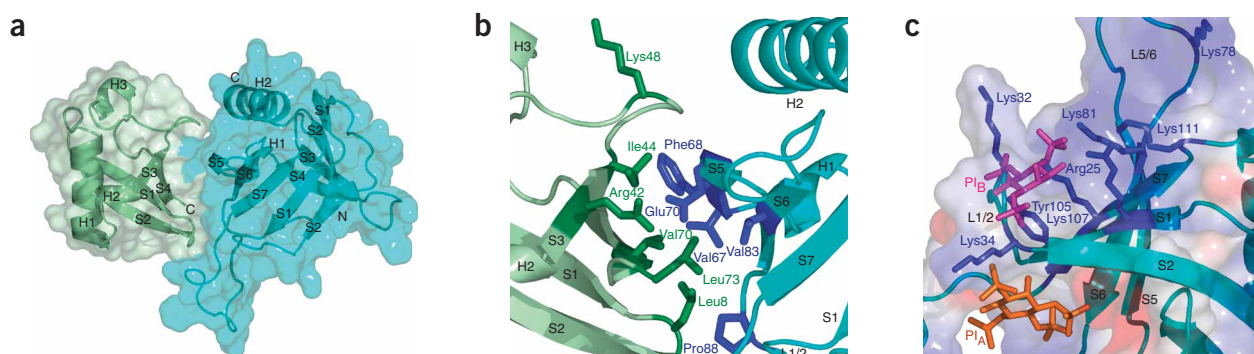


**Figure 1** Structure of the EAP45 GLUE–Ub complex. (a) Ribbon and space-filling model of the complex, with the EAP45 GLUE molecule shown in cyan. (b) Expanded view of the Ub Ile44–EAP45 binding interface (orientation is similar to a). (c) Expanded view showing the approximate locations of the canonical (PI<sub>A</sub>, orange) and noncanonical (PI<sub>B</sub>, magenta) PI-binding sites. To identify the different PI-binding sites, the EAP45 GLUE structure was overlaid onto the PH domain complexes DAPP1/PHISH–I(1,3,4,5)P<sub>4</sub> (PDB 1FAO, secondary structure r.m.s. deviation = 2.8 Å, canonical PI-binding site)<sup>14</sup> and  $\beta$ -spectrin–I(1,4,5)P<sub>3</sub> (PDB 1BTN, secondary structure r.m.s. deviation = 3.4 Å, noncanonical PI-binding site)<sup>15</sup>. The DAPP1 and  $\beta$ -spectrin backbones were then removed for clarity. Basic side chains in the binding site are shown explicitly, and the translucent space-filling model is color coded according to electrostatic potential (dark blue to red, +5 to –5  $k_B T e_c^{-1}$ ).

<sup>1</sup>Department of Biochemistry, University of Utah, Salt Lake City, Utah 84112-5650, USA. <sup>2</sup>Biology Department, 463 Brookhaven National Laboratory, Upton, New York 11973-5000, USA. Correspondence should be addressed to C.P.H. (chris@biochem.utah.edu) or W.I.S. (wes@biochem.utah.edu).

Received 26 July; accepted 2 October; published online 22 October 2006; doi:10.1038/nsmb1160

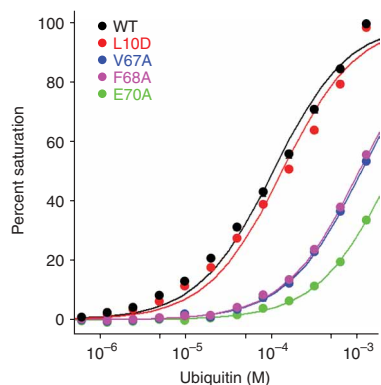


**Figure 2** Biosensor binding analyses of the EAP45 GLUE-Ub interaction. Isotherms show Ub binding to wild-type and mutant EAP45 GLUE proteins (see inset for color coding). Measured  $K_d$  values ( $\mu\text{M}$ ) were as follows: wild-type protein = 105  $\mu\text{M}$ ; L10D = 133; V67A > 1,000; F68A > 1,000; E70A > 1,000. Error bars from triplicate measurements were smaller than the data points.

including Ile44, Leu73 and Leu8, whereas the EAP45 GLUE binding interface is centered about Phe68 and is comprised of residues from S5, S6, H2 and the S6-S7 loop (Fig. 1b). The interface core is hydrophobic on both sides, with peripheral hydrophilic side chain interactions, including Ub Arg42-EAP45 Glu70 (salt bridge) and possibly Ub Lys48-EAP45 Thr127 (hydrogen bond). Several key interacting residues are not conserved in yeast Vps36p, consistent with the idea that yeast ESCRT-II instead binds Ub through an NZF domain (Supplementary Figs. 1 and 2).

In the two crystal forms examined, each EAP45 GLUE domain makes similar contacts with two different ubiquitin molecules, one through the primary binding site described above and a second through an interface centered about EAP45 residue Leu10. Several Ub-binding domains (UBDs) have recently been shown to bind two Ub molecules<sup>10,11</sup>, and we therefore tested the relevance of both crystallographic EAP45 GLUE interfaces for Ub binding in solution. Ub bound the immobilized wild-type EAP45 GLUE domain with a dissociation constant of  $\sim 100 \mu\text{M}$ , which matches the binding energies of many other UBD-Ub interactions (see Fig. 2 and Supplementary Table 2 online for full details)<sup>12</sup>. Mutation of any of the three key residues in the primary EAP45 GLUE binding interface (V67A, F68A or E70A) reduced the Ub-binding affinity more than ten-fold (Fig. 2). Similarly, a single point mutation in the primary Ub-binding surface (I44A) also reduced EAP45 GLUE binding affinity up to 20-fold (Supplementary Table 2). In contrast, a mutation in the center of the second EAP45 GLUE-Ub crystallographic interface (L10D) did not reduce the Ub-binding affinity appreciably. These data all support the idea that the primary interface seen in the EAP45 GLUE-Ub crystal structure forms in solution, whereas the second interface does not.

Like many other PH domains, the GLUE domains from EAP45 and Vps36p also bind inositol phosphates/phosphatidylinositides (abbreviated PI)<sup>5,6</sup>, and the yeast protein binds preferentially to liposomes containing PI(3)P (ref. 6), which is the predominant endosomal PI<sup>13</sup>. PH domains can bind PI ligands at two distinct sites: a canonical site located between the S1-S2 and S3-S4 loops (PI<sub>A</sub> in Fig. 1c) and a noncanonical site located on the other side of the S1-S2 loop, in a pocket between the S1-S2 and S5-S6 loops (PI<sub>B</sub> in Fig. 1c). An overlay of the EAP45 GLUE structure onto PH-PI

complexes from DAPP1 (canonical PI site) and  $\beta$ -spectrin (noncanonical PI site) illustrates that the noncanonical site in EAP45 GLUE forms an extended groove surrounded by basic residues, whereas the canonical site is actually slightly acidic. The EAP45 GLUE structure therefore indicates that PIs probably bind in the noncanonical site (PI<sub>B</sub>), in good agreement with a recent mutational analysis of the Vps36p GLUE domain<sup>6</sup>. *In vitro*, the mammalian EAP45 GLUE domain preferentially binds phosphorylated 3-phosphoinositides such as PI(3,4,5)P<sub>3</sub> (ref. 5), and this apparent difference between the human and yeast proteins may reflect the presence of three additional basic residues in the human EAP45 PIP-binding site (Arg25, Lys34 and Lys107; see Fig. 1c and Supplementary Figs. 1 and 2).

In summary, we find that EAP45 GLUE adopts a split PH domain fold that couples the recognition of ubiquitinated cargoes and endosomal membranes. PIs appear to bind in the noncanonical site at the apex of the  $\beta$ -sandwich, whereas ubiquitin binds along the opposite edge of the second sheet. It appears possible that EAP45 GLUE could bind Ub and PIs cooperatively, as the two binding sites are physically linked through the intervening S5-S6  $\beta$ -hairpin. We speculate that in the absence of ligand binding, the extended insertion that splits the EAP45 GLUE domain between strands S6 and S7 could act as a hinge that allows the S5-S6 hairpin to sample both closed (ligand binding) and open (nonbinding) conformations. Although speculative, such an allosteric binding model is consistent with suggestions that PH domain splitting may support regulated phospholipid binding in other biological systems<sup>7,8</sup>.

**Accession codes.** Protein Data Bank: Coordinates and structure factors have been deposited with accession code 2HTH. Research Collaboratory for Structural Bioinformatics: 038741.

*Note:* Supplementary information is available on the Nature Structural & Molecular Biology website.

#### ACKNOWLEDGMENTS

Biosensor analyses, protein sequencing and mass spectrometry were performed at University of Utah core facilities, and we also thank I. Jafri for technical assistance. This work was supported by US National Institutes of Health grants to C.P.H. (GM66521) and W.I.S. (AI51174). The National Synchrotron Light Source is funded by the US National Center for Research Resources, by the US Department of Energy, Office of Basic Energy Sciences and by the US National Institutes of Health.

#### COMPETING INTERESTS STATEMENT

The authors declare that they have no competing financial interests.

Published online at <http://www.nature.com/nsmb/>

Reprints and permissions information is available online at <http://npg.nature.com/reprintsandpermissions/>

- Hurley, J.H. & Emr, S.D. *Annu. Rev. Biophys. Biomol. Struct.* **35**, 277–298 (2006).
- Sundquist, W.I. *et al. Mol. Cell* **13**, 783–789 (2004).
- Teo, H., Vepritssev, D.B. & Williams, R.L. *J. Biol. Chem.* **279**, 28689–28696 (2004).
- Alam, S.L. *et al. EMBO J.* **23**, 1411–1421 (2004).
- Slagsvold, T. *et al. J. Biol. Chem.* **280**, 19600–19606 (2005).
- Teo, H. *et al. Cell* **125**, 99–111 (2006).
- Lemmon, M.A. *Cell* **120**, 574–576 (2005).
- Yan, J. *et al. EMBO J.* **24**, 3985–3995 (2005).
- Wen, W., Yan, J. & Zhang, M. *J. Biol. Chem.* **281**, 12060–12068 (2006).
- Trempe, J.F. *et al. EMBO J.* **24**, 3178–3189 (2005).
- Hirano, S. *et al. Nat. Struct. Mol. Biol.* **13**, 272–277 (2006).
- Hicke, L., Schubert, H.L. & Hill, C.P. *Nat. Rev. Mol. Cell Biol.* **6**, 610–621 (2005).
- Birkeland, H.C. & Stenmark, H. *Curr. Top. Microbiol. Immunol.* **282**, 89–115 (2004).
- Ferguson, K.M. *et al. Mol. Cell* **6**, 373–384 (2000).
- Hyvonen, M. *et al. EMBO J.* **14**, 4676–4685 (1995).

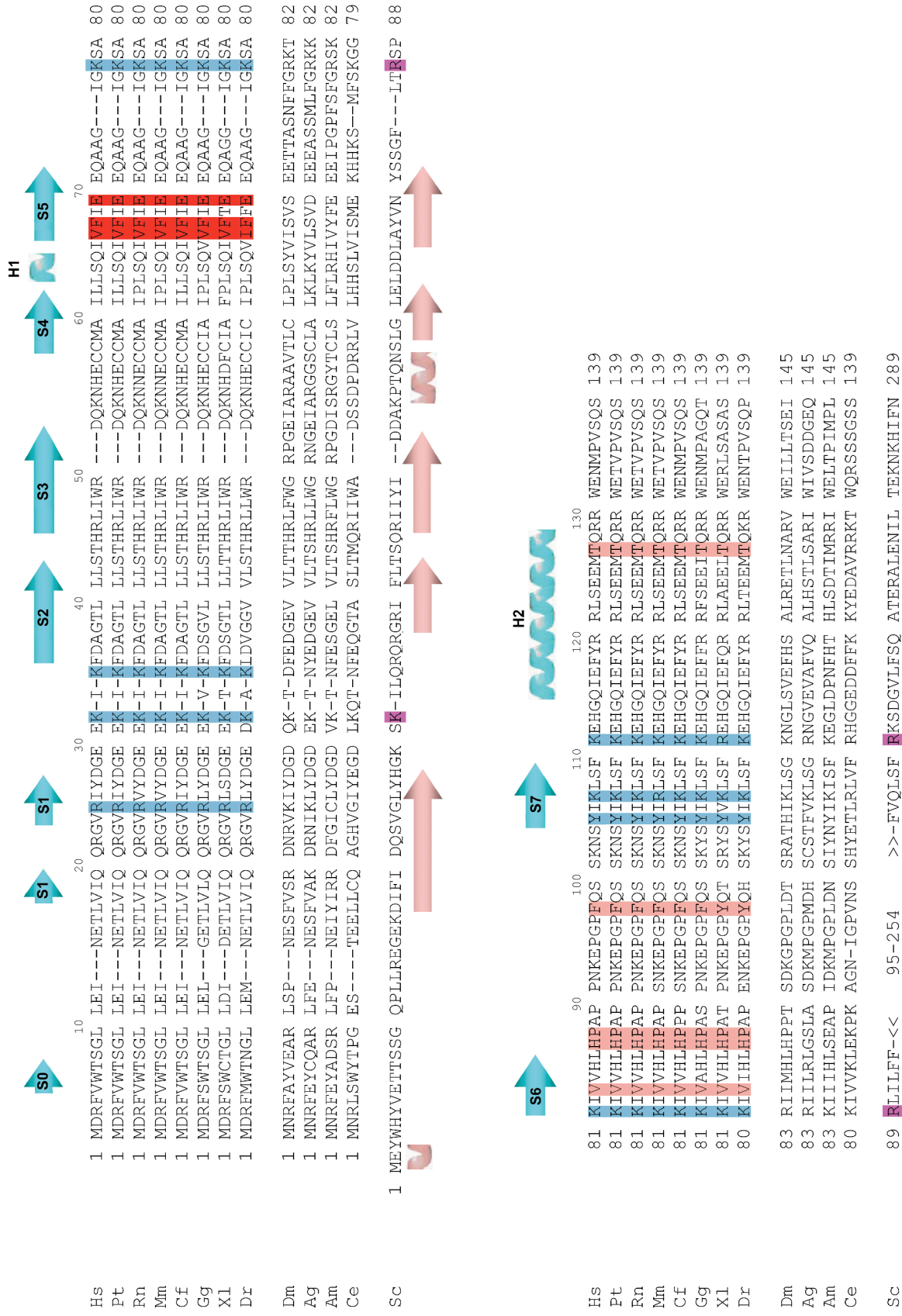


**Fig. S1.** Alignment of EAP45/Vps36p GLUE domains from vertebrates (top), other multicellular eukaryotes (middle) and *S. cerevisia* (bottom). The secondary structures of the human and yeast<sup>13</sup> EAP45/Vps36p GLUE domains are shown above and below. Note that EAP45 S1 is not a continuous  $\beta$ -strand, but is designated as a single strand following the conventions used to describe other PH domains. Residues highlighted in red contact ubiquitin in the EAP45 GLUE:Ub structure, and residues highlighted in dark red were shown experimentally to be required for full Ub binding affinity (see Fig. 2 and Table S2 online). Residues highlighted in light blue constitute the apparent PI binding site (see Fig. 1C), and residues highlighted in magenta were shown experimentally to be required for full affinity PI(3)P binding by the yeast Vps36p GLUE domain. Abbreviations: Hs, *Homo sapiens*, Pt, *Pan troglodytes*, Rn, *Rattus norvegicus*, Mm, *Mus musculus*, Cf, *Canis familiaris*, Gg, *Gallus gallus*, Xi, *Xenopus laevis*, Dr, *Danio rerio*, Dm, *Drosophila melanogaster*, Ag, *Anopheles gambiae*, Am, *Apis mellifera*, Ce, *Caenorhabditis elegans*, Sc, *Saccharomyces cerevisiae*. Primary sequence alignments were created using the clustal W (1.82) multiple sequence alignment algorithm (<http://www.ebi.ac.uk/clustalw/>), except for the Sc sequence, which was aligned based upon the 3D structures of the Hs and Sc proteins. The break in the Sc sequence corresponds to the ~150 amino acid insertion in the split PH domain structure.

**References**

<sup>13</sup>. Teo, H., Gill, D.J., Sun, J., Perisic, O., Veprincev, D.B., Vallis, Y., Emr, S.D. & Williams, R.L., Cell 125, 99-111 (2006).



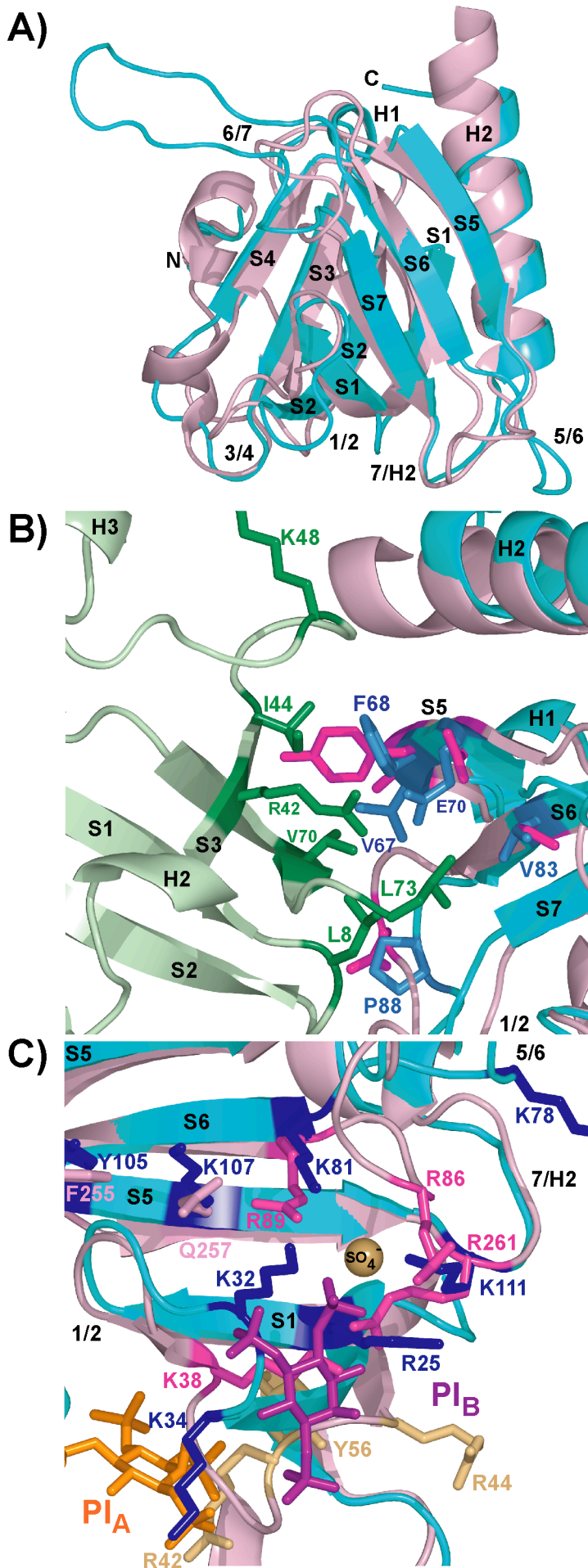


**Fig. S2.** Comparisons of the human EAP45 and yeast Vps36p GLUE domains. **(A)** Superposition of human EAP45 (turquoise) and yeast Vps36p (pink) GLUE domains. **(B)** Expanded view of the Ub I44:EAP45 GLUE binding interface, with yeast Vps36p GLUE (pink) superimposed on EAP45 GLUE (turquoise) to illustrate differences between the EAP45 surface, which binds ubiquitin, and the Vps36p surface which apparently does not. Key interface residues are shown explicitly for Ub (green) and EAP45 GLUE (blue), and the equivalent residues in Vps36p GLUE are shown in magenta. Several key EAP45 GLUE Ub binding residues are not conserved in yeast Vps36p GLUE: EAP45 V67: Vps36p A75, EAP45 F68: Vps36p Y76, EAP45 E70: Vps36p N78 and that buttressing residues in the EAP45 GLUE S6/S7 loop (V83, H87, P88) are apparently missing owing to the larger insertion in the Vps36p protein. Note also that the EAP45 GLUE V67A mutation alone reduced Ub binding affinity more than 10-fold (Fig. 1 and Supplemental Table 2 online).

**(C)** Expanded view showing the approximate locations of the canonical (PIA, orange) and non-canonical (PIB, dark magenta) phosphatidylinositol binding sites in the superimposed EAP45 GLUE and yVps36p GLUE domains. The PI molecules were positioned as described in Fig. 1C, and the color coding is the same as in panels A and B. Residues in Vps36p GLUE required for full affinity phospholipid binding<sup>13</sup> are shown in magenta, additional residues in the apparent PI binding site are shown in pink, the position of a bound sulfate ion is shown in tan, and residues that can be mutated without loss of PI binding are shown in straw. Key residues in the apparent PI binding site of EAP45 GLUE are shown in blue. Note that a series of residues surrounding the non-canonical (PIB) site are conserved as basic residues in both the yeast and human proteins: EAP45 K32: Vps36p K38, EAP45 K78: Vps36p R86, EAP45 K81: Vps36p R89, EAP45 K111: Vps36p R261. The human protein also has three additional basic residues in this region (R25, K35, K107) that may account for the apparent preference of the human protein for more highly phosphorylated forms of 3-phosphoinositides such as PI(3,4,5)P3<sup>14</sup>.

### References

13. Teo, H., Gill, D.J., Sun, J., Perisic, O., Veprentsev, D.B., Vallis, Y., Emr, S.D. & Williams, R.L., *Cell* 125, 99-111 (2006).
14. Slagsvold, T., Aasland, R., Hirano, S., Bache, K.G., Raiborg, C., Trambaiolo, D., Wakatsuki, S. & Stenmark, H., *J Biol Chem* 280, 19600-6 (2005).

**Supplemental Table 1: Data Collection and Refinement Statistics for the EAP45 GLUE:Ub Complex**

	Native	SeMet
<b>Data collection</b>		
Space group	P4 <sub>2</sub> 2 <sub>1</sub> 2	P4 <sub>1</sub> 2 <sub>1</sub> 2
Cell dimensions: <i>a</i> , <i>c</i> (Å)	102.7, 54.3	79.9, 108.7
Wavelength (Å)	1.1	0.9791
Resolution (Å)	50-2.7 (2.77-2.70) <sup>a</sup>	50-3.1 (3.21-3.10) <sup>a</sup>
<i>R</i> <sub>sym</sub>	0.11 (0.54)	0.12 (0.53)
<i>I</i> / <i>σ</i> ( <i>I</i> )	19.9 (1.9)	17(3.1)
Completeness (%)	97.7 (81.4)	100.0 (100.0)
Redundancy	25.8	15.2
<b>Refinement</b>		
Resolution (Å)	50-2.7 (2.77-2.70) <sup>a</sup>	
No. unique reflections	8236(489) <sup>a</sup>	
<i>R</i> <sub>work</sub> / <i>R</i> <sub>free</sub> <sup>b</sup>	0.248/0.289	
No. atoms	1,641	
Protein	1,641	
<i>B</i> -factors (Å <sup>2</sup> ): Protein	56.3	
r.m.s deviations		
Bond lengths (Å)	0.018	
Bond angles (°)	1.681	

Native and SeMet data were each collected from single crystals.

<sup>a</sup>Values in parentheses refer to the high-resolution shell.

<sup>b</sup>R<sub>free</sub> was calculated with a randomly selected test set of 810(9.8%) reflections.

**Supplemental Table 2.** Binding Affinities of Different EAP45 GLUE:Ub Complexes.

<b>EAP45 GLUE Mutants</b>	<b>Ub <math>K_D^a</math> (<math>\mu</math>M)</b>	<b>Temp</b>	<b>Buffer</b>
WT	209 (1) <sup>c</sup>	4°C	Phosphate
V67A	1090 (30) <sup>c</sup>		Phosphate
F68A	1060 (20) <sup>c</sup>		Phosphate
E70A	1500 (45) <sup>c</sup>		Phosphate
L10D	228 (3) <sup>c</sup>		Phosphate
WT	411 $\pm$ 95 <sup>b</sup>	20°C	Phosphate
V67A	2120 $\pm$ 720 <sup>b</sup>		Phosphate
F68A	1570 $\pm$ 950 <sup>b</sup>		Phosphate
E70A	2050 $\pm$ 1830 <sup>b</sup>		Phosphate
L10D	506 (9) <sup>c</sup>		Phosphate
WT	105 (3) <sup>c</sup>	4°C	Tris
V67A	>1000 <sup>d</sup>		Tris
F68A	>1000 <sup>d</sup>		Tris
E70A	>1000 <sup>d</sup>		Tris
L10D	133 (1) <sup>c</sup>		Tris
WT	261 (6) <sup>c</sup>	20°C	Tris
V67A	>1000 <sup>d</sup>		Tris
F68A	>1000 <sup>d</sup>		Tris
E70A	>1000 <sup>d</sup>		Tris
L10D	405 (40) <sup>c</sup>		Tris
<b>Ubiquitin Mutants</b>			
GST-EAP45 <sub>1-139</sub> : Ub	411 $\pm$ 95 <sup>b</sup>	20°C	Phosphate
GST-EAP45 <sub>1-139</sub> : Ub I44A	>1000 (100) <sup>cd</sup>	20°C	Phosphate
GST-EAP45 <sub>1-139</sub> : Ub F4A	392 (9) <sup>c</sup>	20°C	Phosphate
GST-Ub : EAP45 <sub>1-139</sub>	66 $\pm$ 8 <sup>b</sup>	4°C	Tris
GST-Ub I44A : EAP45 <sub>1-139</sub>	>1000 <sup>d</sup>	4°C	Tris

<sup>a</sup> $K_D$  values were determined in Biacore biosensor measurements of soluble protein ligand binding to immobilized GST fusion proteins at the indicated temperature in either Phosphate buffer (20 mM sodium phosphate, 150 mM NaCl, 5 mM  $\beta$ -ME, 0.01% P20, 0.2 mg/mL BSA, pH 7.2) or Tris buffer (20 mM Tris, 150 mM NaCl, 1 mM DTT, 0.01% P20, 0.2 mg/mL BSA, pH 8.0). Note that several of these measurements were reported previously<sup>1</sup>, but are also included here for completeness.

<sup>b</sup>Dissociation constant is the mean of two or more independent measurements and the error is the standard deviation in the measurements.

<sup>c</sup>Dissociation constant and error were estimated from a statistical fit of a single binding isotherm derived from triplicate measurements of 10 different soluble protein ligand concentrations. Values in parentheses are statistical errors estimated from the fit of the data to a simple 1:1 binding model.

<sup>d</sup>Extrapolated from less than 50% saturation binding.

# Structural basis for ubiquitin recognition by the human EAP45/ESCRT-II GLUE domain

Steven L. Alam<sup>1</sup>, Charles Langelier<sup>1</sup>, Frank G. Whitby<sup>1</sup>, Sajjan Koirala<sup>1</sup>, Howard Robinson<sup>2</sup>, Christopher P. Hill<sup>1</sup>, & Wesley I. Sundquist<sup>1</sup>

<sup>1</sup>*Department of Biochemistry, University of Utah, Salt Lake City, UT 84112-5650, USA.*

<sup>2</sup>*Biology Department, 463 Brookhaven National Laboratory, Upton, New York 11973-5000. Correspondence should be addressed to CPH or WIS [chris@biochem.utah.edu](mailto:chris@biochem.utah.edu), [wes@biochem.utah.edu](mailto:wes@biochem.utah.edu).*

## SUPPLEMENTAL MATERIAL

### Experimental Procedures

#### Protein Expression and Purification

The GLUE domain of human EAP45 was expressed as a GST-fusion (GST-EAP45<sub>1-139</sub>) using a modified pGEX2T vector (WISP01-69) that incorporated a TEV cleavage site between GST and the cloned protein<sup>1</sup>. Site directed mutagenesis was carried out using the QuickChange<sup>TM</sup> method (Stratagene). Proteins were expressed in BL21(DE3) Codon Plus RIPL cells (Stratagene) by one of two methods: 1) cells were grown in terrific broth and induced with 0.5 mM IPTG for 12 h at 13°C, or 2) cultures were grown at 37°C from single colonies in autoinduction media<sup>2</sup>, switched to 13°C after 5-8 hours, and allowed to grow for an additional 12 h. Selenomethionine (SeMet) EAP45 GLUE was expressed using autoinduction media supplemented with SeMet<sup>2</sup>.

All steps in the purification were performed at 4°C. Cells from 6 l cultures were pelleted, resuspended in 300 ml buffer A (50mM Tris pH=8.0, 150mM NaCl, 1mM DTT) and a cocktail of protease inhibitors (aprotinin, PMSF, leupeptin, and pepstatin), 5% glycerol, 0.5% NP-40, plus 75 mg lysozyme, lysed by sonication, and the extracts were centrifuged at 18,000 x g for 45 minutes. The clarified extracts were loaded onto a glutathione affinity column (GST Prep FF 26/10) equilibrated with buffer A, washed with three column volumes of buffer A, and eluted with buffer B (50mM Tris pH=8.0, 150mM NaCl, 1mM DTT plus 20 mM reduced glutathione). Fractions containing GST-EAP45<sub>1-139</sub> were pooled, supplemented with TEV protease (200 U),



dialyzed for 72 h vs. buffer C (20mM Tris pH=8.0, 100mM NaCl, 1mM DTT and 0.5mM EDTA), and concentrated to 30 ml. The protein was then purified further by anion exchange (Q-sepharose FF 26/10) equilibrated in buffer C lacking EDTA. Flow-through fractions containing the cleaved EAP45 GLUE domain were pooled, concentrated to 3 ml, and purified to homogeneity by size exclusion chromatography (Sephadex75 16/60) in buffer D (20mM Tris pH=8.0, 150mM NaCl, 1mM DTT). The purity and composition were confirmed by SDS-PAGE and mass spectrometry, and the protein was concentrated to 500  $\mu$ M for crystallization trials and Biacore experiments. This procedure typically yielded 5-10 mg of pure EAP45 GLUE. TEV protease cleavage resulted in two non-native N-terminal amino acids (His-Gly), but our residue numbering scheme corresponds to that of the native protein.

The ubiquitin expression construct was a generous gift from the late Cecile Pickart (Johns Hopkins University). Recombinant Ub and mutants were expressed and purified as described previously<sup>3</sup>.

### **Crystallization and Data Collection**

Ub (500  $\mu$ M) was mixed in a 1:1 ratio with native or SeMet EAP45 GLUE in buffer D. EAP45 GLUE:Ub complexes were crystallized at 4°C by the sitting drop vapor diffusion method after mixing equal volumes (2  $\mu$ l) of protein complex solution and well solution (10% ethylene glycol, 10.5% PEG8000, and 100mM Hepes pH=7.5). Both the native and SeMet proteins crystallized in two different, but related, crystal forms. Crystals were transferred to a cryoprotectant solution containing precipitant supplemented with 30% ethylene glycol and flash frozen in liquid nitrogen prior to data collection. Data were collected and the structure was initially solved using a selenomethionine crystal in space group P4<sub>1</sub>2<sub>1</sub>2 (a=80.2Å, b=80.2Å, c=110.2 Å). However, the best diffracting crystal was from native protein crystal in space group p4<sub>2</sub>2<sub>1</sub>2 (a=102.7 Å, b=102.7Å, c=54.3Å).

X-ray diffraction data were collected at Brookhaven National Lab (BNL) at beamline X29. Single-wavelength anomalous dispersion (SAD) data (3.1 Å resolution) were collected from a Se-Met EAP45 GLUE:Ub crystal (0.9791Å), and native (2.7 Å resolution) data set were collected from a native crystal. The data were processed using HKL<sup>4</sup>.

### **Structure Determination and Refinement**

The SeMet EAP45 GLUE structure was initially determined using the SAD method<sup>5-7</sup>. SOLVE and RESOLVE were used to locate and refine the positions for 3 of 4 possible selenomethionine sites<sup>8</sup>. Phases were calculated and used to produce a 3.1Å electron density map. An Ub model was initially docked into the electron density and the EAP45 GLUE model was built *de novo* in O<sup>9</sup>. The model was refined against the SeMet data using REFMAC from the CCP4 suite<sup>10</sup>. The refined SeMet model was then used as an initial search model for a molecular replacement solution of the native dataset using MOLREP. The model was then rebuilt in O and refined in REFMAC.

A single EAP45:Ub complex occupied the asymmetric unit in both crystal forms. Both forms showed the same two major EAP45 GLUE:Ub contacts, and differed primarily in the orientation of a homomeric Ub:Ub packing interface. Only the higher resolution native data set is described herein, and statistics for the structure determination are given in Supplemental Table 1. The following terminal and loop residues of EAP45 GLUE were poorly ordered and therefore included at zero occupancy: 1-2 (N-terminus), 32-36 (S1/S2 loop), 53-57 (S2/S3 loop), 74-78 (S4/S5 loop), 92-103 (S6/S7 loop).

### **Biosensor Binding Experiments**

Biosensor binding experiments were performed to characterize the EAP45 GLUE:Ub interaction in solution. Experiments were performed at both 4°C and 20°C using a BIACORE

2000 (Biacore AB, Uppsala, Sweden) equipped with a research-grade CM4 sensor chip. Approximately 5000 response units (5 kRU) anti-GST antibody was immobilized on flow cells using amine-coupling chemistry<sup>11</sup>. GST-EAP45<sub>1-139</sub>, GST-EAP45<sub>1-139</sub>V67A, GST-EAP45<sub>1-139</sub>F68A, GST-EAP45<sub>1-139</sub>E70A, GST-Ub, GST-Ub I44A, or GST alone from soluble *E. coli* lysates were diluted in running buffer (20 mM sodium phosphate, 150 mM NaCl, 5 mM  $\beta$ -ME, 0.01% P20, 0.2 mg/mL BSA, pH 7.2 or 20 mM Tris, 150 mM NaCl, 1 mM DTT, 0.01% P20, 0.2 mg/mL BSA, pH 8.0) and captured on the antibody surfaces at densities of ~0.5 kRU. Pure GST alone was also captured as a blank reference. In one set of experiments, Ub and Ub I44A were purified, diluted in running buffer, and injected in triplicate over the immobilized EAP45<sub>1-139</sub> proteins at concentrations of 0-2500  $\mu$ M. Equilibrium binding isotherms were fit to simple 1:1 binding models to determine the dissociation constant and statistical fitting errors<sup>12</sup>. Experiments were also performed in the reverse orientation by flowing purified EAP45<sub>1-139</sub> (0-500  $\mu$ M) over immobilized GST-Ub proteins. All of the binding experiments were performed at both 4°C and 20°C because EAP45<sub>1-139</sub> proteins tended to aggregate at elevated temperatures. Binding measurements were also performed in both phosphate buffer (20 mM sodium phosphate, 150 mM NaCl, 5 mM  $\beta$ -ME, 0.01% P20, 0.2 mg/mL BSA, pH 7.2) and Tris buffer (20 mM Tris, 150 mM NaCl, 1 mM DTT, 0.01% P20, 0.2 mg/mL BSA, pH 8.0). Data shown in Fig. 2 are for measurements made in Tris buffer at 4°C. Dissociation constants for all interactions examined are summarized in **Supplemental Table 2** online.

## References

1. Langelier, C., von Schwedler, U., Fisher, R.D., De Domenico, I., White, P.L., Hill, C.P., Kaplan, J., Ward, D. & Sundquist, W.I. The Human ESCRT-II Complex and Its Role in HIV-1 Release. *J. Virol.* **80**, 9465-9480 (2006).
2. Studier, F.W. Protein production by auto-induction in high density shaking cultures. *Protein Expr Purif* **41**, 207-34 (2005).
3. Beal, R., Deveraux, Q., Xia, G., Rechsteiner, M. & Pickart, C. Surface hydrophobic residues of multiubiquitin chains essential for proteolytic targeting. *Proc Natl Acad Sci U S A* **93**, 861-6 (1996).
4. Otwinowski, Z. & Minor, W. Processing of X-ray diffraction data collected in oscillation mode. *Methods in Enzymol.* **276**, 307-326 (1997).
5. Yu-dong, L., Harvey, I., Yuan-xin, G., Chao-de, Z., Yi-zong, H., Hai-fu, F., Hasnain, S.S. & Hao, Q. Is single-wavelength anomalous scattering sufficient for solving phases? A comparison of different methods for a 2.1 Å structure solution. *Acta Crystallogr D Biol Crystallogr* **55**, 1620-2 (1999).
6. Dauter, Z., Dauter, M. & Dodson, E. Jolly SAD. *Acta Crystallogr D Biol Crystallogr* **58**, 494-506 (2002).
7. Dodson, E. Is it jolly SAD? *Acta Crystallogr D Biol Crystallogr* **59**, 1958-65 (2003).
8. Terwilliger, T.C. Automated structure solution, density modification and model building. *Acta Crystallogr D Biol Crystallogr* **58**, 1937-40 (2002).
9. Jones, T.A., Zou, J.Y., Cowan, S.W. & Kjeldgaard. Improved methods for binding protein models in electron density maps and the location of errors in these models. *Acta Crystallogr A* **47 (Pt 2)**, 110-9 (1991).
10. Murshudov, G.N., Vagin, A.A., Lebedev, A., Wilson, K.S. & Dodson, E.J. Efficient anisotropic refinement of macromolecular structures using FFT. *Acta Crystallogr D Biol Crystallogr* **55 (Pt 1)**, 247-55 (1999).
11. Johnsson, B., Lofas, S. & Lindquist, G. Immobilization of proteins to a carboxymethyl-dextran-modified gold surface for biospecific interaction analysis in surface plasmon resonance sensors. *Anal Biochem* **198**, 268-77. (1991).
12. Myszka, D.G. Improving biosensor analysis. *J Mol Recognit* **12**, 279-84. (1999).
13. Teo, H., Gill, D.J., Sun, J., Perisic, O., Veprintsev, D.B., Vallis, Y., Emr, S.D. & Williams, R.L. ESCRT-I Core and ESCRT-II GLUE domain structures reveal role for GLUE in linking to ESCRT-I and membranes. *Cell* **125**, 99-111 (2006).
14. Slagsvold, T., Aasland, R., Hirano, S., Bache, K.G., Raiborg, C., Trambaiolo, D., Wakatsuki, S. & Stenmark, H. *J Biol Chem* **280**, 19600-6 (2005).